Delft University of Technology

Coreflood Study of Non-Monotonic Fractional-Flow Behavior with Foam: Implications for Surfactant-Alternating-Gas Foam EOR

Salazar Castillo, Rodrigo; Rossen, Bill

Citation (APA)
Salazar Castillo, R., & Rossen, B. (2019). Coreflood Study of Non-Monotonic Fractional-Flow Behavior with Foam: Implications for Surfactant-Alternating-Gas Foam EOR. In *IOR 2019 � 20th European Symposium on Improved Oil Recovery* Article Tu A 11 EAGE. https://doi.org/10.3997/2214-4609.201900109

Important note
To cite this publication, please use the final published version (if applicable).
Please check the document version above.

Tu A 11

Coreflood Study of Non-Monotonic Fractional-Flow Behavior with Foam: Implications for Surfactant-Alternating-Gas Foam EOR

R.O. Salazar Castillo[1]*, W. Rossen[1]

[1]TU Delft

Summary

Foam is able to increase gas's sweep efficiency in Enhanced-Oil-Recovery applications. A surfactant-alternating-gas, or SAG, process is usually preferred for placing foam in the reservoir. During a SAG process, foam is generated away from the wellbore, offering both good injectivity and good mobility control at the leading edge of the foam bank.

Scale-up of laboratory data for SAG to field applications remains a challenge. Direct scale-up of dynamic SAG coreflood results is unreliable because of the dominance of core-scale artifacts. Steady-state coreflood data can be scaled up using fractional-flow theory (Kibodeaux and Rossen, 1997; Rossen and Boeije, 2015). However, about half the published laboratory studies of foam fractional-flow curves report non-monotonic behavior, where at some point liquid saturation Sw increases with decreasing liquid fractional flow fw. Rossen and Bruining (2007) warn that such behavior would result in foam collapse during injection of the gas slug in a SAG process at the field scale. Here we report and analyse a series of steady-state and dynamic coreflood experiments to investigate the occurrence of non-monotonic fractional-flow behavior. These corefloods vary surfactant concentration, injected gas fraction (foam quality) and total superficial velocity and are supported by CT measurements. The CT data confirm that in these cases, as foam weakens with decreasing fw, liquid saturation increases, confirming the non-monotonic fw(Sw) behaviour.

In our results, every case of non-monotonic fractional-flow behavior begins with propagation of foam from the inlet, followed by eruption of a much-stronger foam at the outlet of the core and backwards propagation of the stronger foam state to the inlet, similar to behavior reported by Apaydin and Kovscek (2001) and Simjoo et al. (2013). This suggests that there may be more than one stable local-equilibrium (LE) foam state. The initial creation of the stronger foam near the outlet is at least in part due to the capillary end effect. It is thus not clear which LE foam state controls behaviour in a SAG process in the field.

In our results, the subsequent transition from a stronger- to a weaker-foam state, leading to non-monotonic fw(Sw) behavior, coincides with conditions for weaker foam (lower surfactant concentration, lower fw) and less-vigorous foam generation (lower superficial velocity); this agrees with the theory of foam propagation of Ashoori et al. (2012). We discuss the implications of these findings, if confirmed to apply generally, for design of SAG foam processes.

Introduction

Foam can improve sweep efficiency in gas-injection enhanced-oil-recovery (EOR) processes (Schramm, 1994; Rossen, 1996). Surfactant-alternating-gas (SAG) injection is the preferred method of placing foam in the reservoir, both for operational and injectivity reasons (Matthews,1989; Heller 1994).

Scale-up of laboratory SAG coreflood data is challenging, because core-scale lengths and times may not be sufficient for foam to reach local equilibrium rapidly enough to scale-up behaviour directly to the field (Kapetas et al., 2014).

Assuming that local equilibrium applies on the field scale, it is possible to scale-up steady-state laboratory coreflood data to field scale using fractional-flow theory (Zhou and Rossen, 1994; Shan and Rossen, 2004; Boeije and Rossen, 2018). Fractional-flow theory teaches that upon injection of a gas slug in SAG there is a shock to a condition of very low water fractional flow f_w. Thus behaviour at low f_w is crucial to foam performance. Figure 1 shows schematically the solution for the displacement as the first gas slug is injected into a reservoir saturated with surfactant solution on a diagram of f_w plotted as a function of water saturation S_w. J represents the injected fluid ($f_w = 0$) and I the initial state ($S_w = 1$). For simplicity we assume here that there is no mobile oil in the near-well region where the displacement takes place. All saturations in the displacement lie at fractional-flow values below the point of tangency representing the shock. Each saturation propagates with dimensionless velocity equal to the slope ($\mathrm{d}f_w/\mathrm{d}S_w$) of the fractional-flow function at that saturation. The monotonic decrease in this slope and as f_w decreases represents the gradual transition between the low-mobility shock and dry conditions, with very high mobility, at the well. This high mobility helps injectivity (Al Ayesh et al., 2017). (Fingering of drier, higher-mobility gas through the lower-mobility gas ahead of it within the foam bank can complicate behaviour (Farajzadeh et al., 2016; Van der Meer et al., 2018); this issue is outside the scope of this paper.) The mobility at the shock (point of tangency in Fig. 1) is crucial. If mobility control is not maintained across the shock (between the point of tangency and I), viscous instability results and in addition gravity segregation of gas worsens.
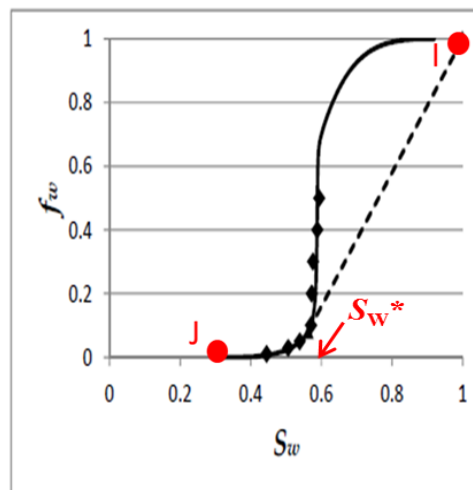

***Figure 1** Construction of displacement by the first gas slug in a SAG process on fractional-flow curve: monotonic* $\mathbf{f_w(S_w)}$ *function. Modified from Boeije and Rossen, 2018.*

Measuring steady-state mobilities at such low values of f_w is challenging. In addition, about half of the studies of the $f_w(S_w)$ function for foam processes find, not a monotonic decrease in S_w as f_w decreases, as in Fig. 1, but an increase in S_w over some range of f_w, and then a reversion to decreasing S_w, as illustrated in Fig. 2. Rossen and Bruining (2007) show that this behaviour then predicts a shock to fully collapsed foam on the bottom branch of the $f_w(S_w)$ curve, as shown in Fig. 2. Mobility control would in such a process would be much less favourable than in a process like that in Fig. 1.
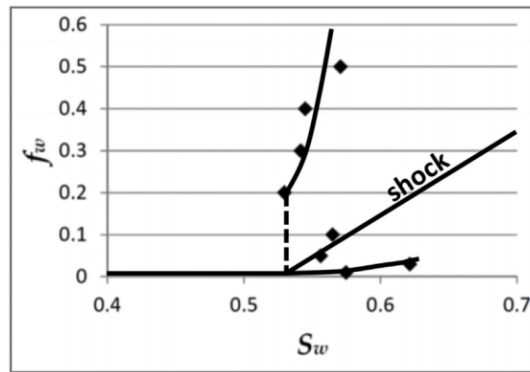
Figure 2 Non-monotonic $f_w(S_w)$ function and construction of displacement by the first gas slug in a SAG process. From Boeije and Rossen, 2018.

In this paper we report part of a study of fractional-flow curves for foam processes, with application to SAG. In several cases, we found monotonic behaviour in the $f_w(S_w)$ function; We are preparing a companion paper describing these cases. In this paper we report on the case with non-monotonic behaviour. In this study, in every case where non-monotonic behaviour was observed, that behaviour started with a laboratory artefact related to the capillary-end effect. In addition, the weakening of foam (increase in S_w and large increase in mobility) with decreasing f_w correlates with factors related either to reduced foam generation or reduced lamella stability. This suggests that the transition to foam can be related to either to a failure of foam generation or reduced foam stability. As seen in other studies (Ashoori et al., 2012; Yu et al., 2019a, b), transitions to weaker or stronger foam states depend on factors related to both foam generation and foam stability. We discuss the implications of these results for scale-up and design of SAG processes to field application.
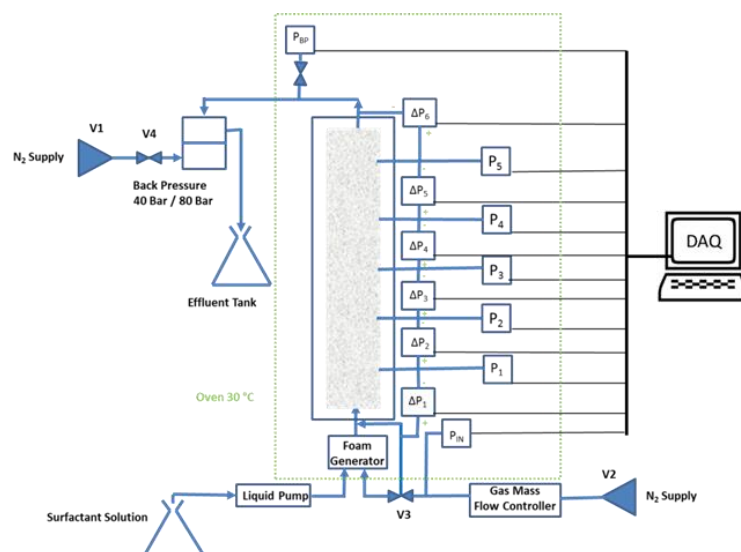

Figure 3 Schematic of experimental apparatus A, with controlled temperature. Apparatus B is substantially similar, with changes noted in the text

Methods

Experimental Apparatus
We conducted coreflood experiments in two apparatuses, A and B. Apparatus A, depicted in Figure 3, is able to co-inject gas (N_2) and surfactant solution over a range of total superficial velocities between 0.82 and 16 ft/day. We injected the liquid phase using a Vindum pump model VP1, which is able to deliver a minimum flow rate accurately as low as 1×10^{-4} mL/min. To inject the gas phase we used a Bronkhorst gas mass-flow controller Model F-033CI which, in combination with a Coriolis flow meter, is able to deliver a flow rate between 1.2 and 60 g/h. A glued core was placed into a PEEK

(polyether ether ketone) core holder with a narrow liquid-filled gap between, pressurized to the injection pressure. We placed the core holder vertically and we injected the fluids from bottom to top. To help achieve steady-state, in some cases we used a foam generator upstream of the core inlet: a PEEK three-way-connector with a build-in micrometric filter. In order to reduce gas expansion along the core, a back-pressure regulator fixed at either 40 or 80 bar was placed at the outlet of the core. Seven absolute-pressure transducers and six differential-pressure transducers were connected using lines filled with liquid, connected to the core, to monitor gas expansion and foam mobility along the core. The apparatus was placed inside an oven maintained at 30°C. Apparatus B is an adaptation of apparatus A to fit in a CT-scanner in order to monitor water saturation during corefloods. The core holder was placed horizontally in the CT-scanner. PEEK lines replaced the metal lines connected to the core holder to reduce the X-ray attenuation. In both apparatuses we digitally recorded the pressure and temperature data every 1.7s using a program coded in Labview.

Materials

During the coreflood experiments we co-injected nitrogen and surfactant solution to generate foam. The nitrogen was supplied by a 200-bar cylinder with a purity of 99.98%. The surfactant solutions consisted of a synthetic brine prepared with demineralized water, 1.0 wt% sodium chloride, and anionic AOS surfactant (Stepan BIO-TERGE AS-40). We prepared four formulations with surfactant concentrations, C_S, of 0.037 wt%, 0.1 wt%, 0.5 wt% and 1.0 wt%, respectively. All these surfactant concentrations are well above the critical micelle concentration, CMC. To clean the core between experiments we used a solution of 50 vol.% tap water and 50 vol.% isopropyl alcohol. The alcohol purity is 99.7%. We used two cylindrical Bentheimer cores cut from the same outcrop. The length of the cores was 38 cm and their diameter 3.8 cm. The measured average permeabilities are 2300 md and 2100 md, respectively. We measured an average porosity of 0.226 for the second core using the CT-scanner.

Experimental Procedure

At the start of each experiment we injected 10 pore volumes (PV) of CO_2 to displace any gas inside the core. Next, we injected at least 10 PV of brine at elevated pressure (80 bars) to dissolve any CO_2 that remained in the core. Then, we measured the liquid permeability of the core. Finally, we injected 10 PV of surfactant solution to satisfy adsorption.

During each experiment we performed one or more foam-quality scans. Foam quality is gas fractional flow, i.e. (1- f_w). A foam scan is a series of steady-state measurements at different f_w and fixed total superficial velocity, u_t. Since our goal is to upscale a gas-injection process in SAG, we focus on data at low f_w. In order to assure that our results are independent of the initial state of the core, we performed steady-state measurements alternating between high and low foam qualities. Between experiments we injected at least 10 PV of gas.

As in other experimental studies (Apaydin and Kovscek, 2001; Simjoo et al., 2013), we observed the eruption of a much stronger foam at the end of the core and subsequent slow upstream propagation of the corresponding foam state. In this paper we report the data after gas breakthrough and allowed for sufficient time for the stronger foam state to propagate through the core. In such cases we report the data from sections 4 and 5 after the entire core has settled into steady-state.

In most experiments we inferred water saturation, S_w, from measured mobility using a estimated water relative-permeability function $k_{rw}(S_w)$ for Bentheimer sandstone (Eftekhari et al., 2017; Kapetas et al., 2018). In one foam scan we monitored S_w using a medical CT scanner. We scanned the core horizontally in slices of 0.2 mm. Details of this procedure can be found, for example, in Eftekhari et al. (2017). From the CT response, we calculated the liquid saturation in each voxel and from that the average in various cross-sections.

At the end of each experiment we cleaned the core as follows, following a procedure similar to that used by Eftekhari et al. (2017) and Kahrobaei et al. (2017) on shorter cores. First, we injected 10 PV of a 50/50 water/isopropyl alcohol solution at elevated pressure (80 bar) to kill foam. Second, we injected 10 PV of water initially at elevated (80 bar) back-pressure, and we reduced pressure slowly to atmospheric in order to allow the expansion of trapped gas. Third, we injected 10 PV of CO_2 followed by an additional 10 PV of water at atmospheric pressure. Fourth, we flushed the core again with 20 PV of water while gradually raising the back-pressure until its value reached 80 bar. Then we gradually reduced pressure to atmospheric. Fifth, we vacuum-cleaned the core, followed by the injection of at least 10 PV of CO_2. Finally, we performed the preparation procedure described above and verified that the core had been restored to its initial permeability.

Results

In this paper, we analyze steady-state data collected after the eruption of stronger foam at the core outlet and the subsequent propagation of this stronger foam state upstream of the core. The plot on the left of Figure 4 depicts the propagation of pre-generated foam downstream through the core, during a foam scan. The nominal foam quality (at back-pressure), nominal total superficial velocity and surfactant concentration are 95%, 2 ft/day and 0.5 wt%, respectively. This foam propagates with nearly uniform pressure gradient ∇p in all sections except the entrance and exit sections. At steady state, foam quality and total superficial velocity varies with gas expansion in the core, but liquid superficial velocity is uniform. At high foam quality, ∇p depends on liquid superficial velocity (Alvarez et al., 2001); thus ∇p in this advancing foam bank agrees with expected local-equilibrium behaviour.

As soon as the flowing foam breaks through to the outlet face of the core at about 1 PV injection, the eruption of a stronger foam starts at the core outlet and propagates upstream; this has just begun in Fig. 4, left. After a longer period of time, the system attains steady-state, illustrated in Figure 4, right. The foam present after breakthrough is considerably less mobile than the foam before foam breakthrough. Also, ∇p is different in all sections in this final configuration: it increases along the core. This behaviour would not be expected in the high-quality regime.
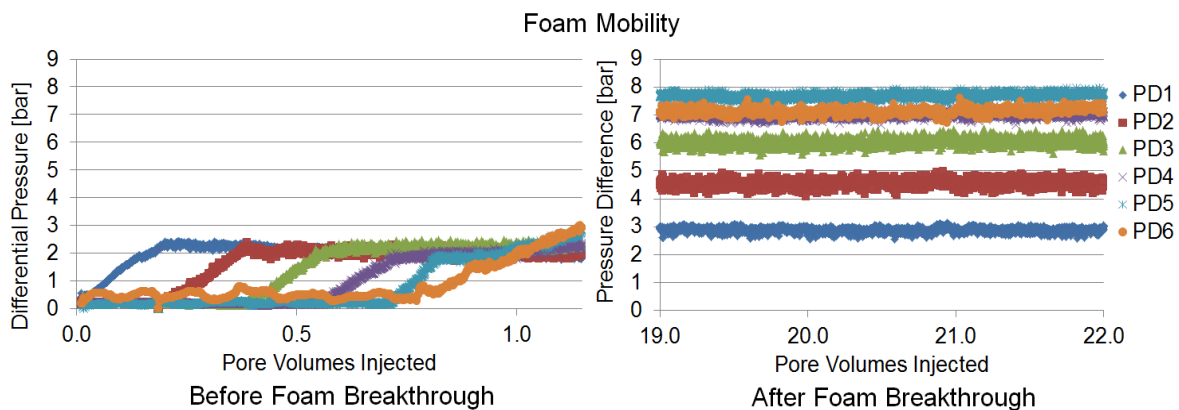

Figure 4 Sectional differential pressures in bars in foam coreflood as function of pore volumes injected. Since all sections have the same length, these values are directly proportional to pressure gradient in each section. On the left, before foam breakthrough. On the right, steady-state pressure difference long after foam breakthrough. The nominal foam quality and total superficial velocity and the surfactant concentration of this experiment are 95%, 2 ft/day and 0.5 wt%, respectively.

In contrast, we did not observe the eruption of stronger foam in a similar experiment under the same experimental conditions but with a higher foam quality (98%). Foam mobility before and after foam breakthrough were practically the same. Steady-state foam is considerably weaker in this case, as depicted in Figure 5.
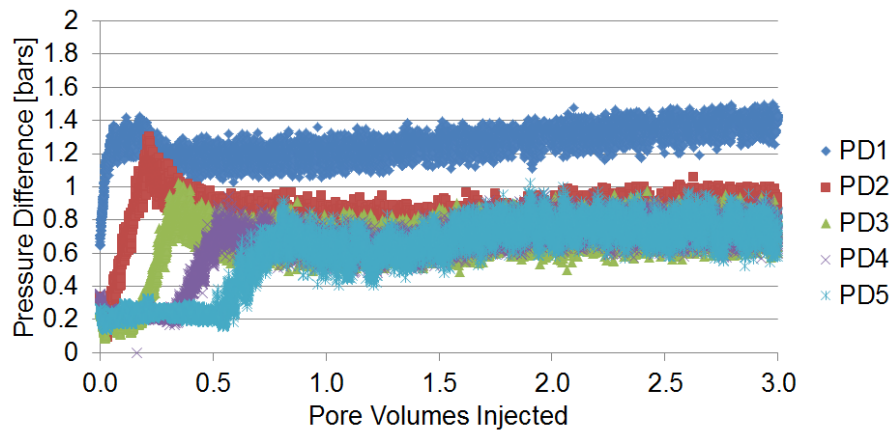
Figure 5 Sectional differential pressures in bars as function of pore volumes injected. The nominal foam quality and total superficial velocity and the surfactant concentration of this experiment are 98%, 2 ft/day and 0.5 wt%, respectively. Breakthrough has no effect on the mobility of foam upstream of the core.
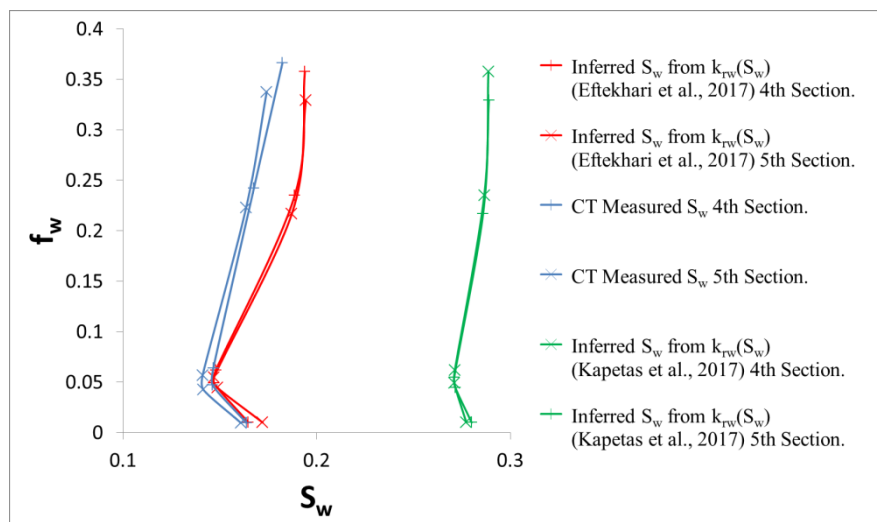

Figure 6 Fractional-flow function $f_w(S_w)$ for a foam scan performed at a total superficial velocity of 4.21 ft/day (1.48 x 10^{-5} m/s) with C_S = 0.5 wt%. The blue curves show S_w as measured directly using a CT scanner. The red curves show S_w as inferred using the $k_{rw}(S_w)$ function reported by Eftekhari et al. (2017). The green curves show S_w as inferred using the $k_{rw}(S_w)$ function reported by Kapetas et al., (2017) based on data with no foam present.

A foam scan focused on the high-quality regime performed at a total superficial velocity of 4.21 ft/day (1.48 x 10^{-5} m/s) with C_S = 0.5 wt% is summarized in Figure 6. The mobilities measured during the foam scan reveal that foam weakened in an unexpected manner as f_w decreased. During this foam scan, we used a CT scanner to monitor water saturation S_w. Our S_w measurements confirm that S_w indeed increased at some point as f_w decreased. This trend can be deduced from pressure-gradient data even using an approximate $k_{rw}(S_w)$ function. The green curves in Figure 6 show S_w calculated from ∇p in two sections using the $k_{rw}(S_w)$ function measured by Kapetas at. (2017) at low capillary number in the absence of foam. The estimated values of S_w are consistently greater than those measured with the CT scanner, but the trend of S_w with decreasing f_w is consistent with the CT data. The larger absolute values of S_w reflects the large value of irreducible water saturation S_{wr} that Kapetas et al. inferred from their fit of data in the absence of foam. Using the $k_{rw}(S_w)$ function measured by Eftekhari et al. (2017) in the presence of foam (red curve in Figure 6) gives a better fit. Though not a quantitatively accurate fit to the CT results, it also fits the trend in the data. Thus, either of this two functions could have been be used to deduce the non-monotonic trend of S_w upon decreasing f_w from ∇p data.

Our experiments suggest that the non-monontonic $f_w(S_w)$ behaviour is due to the eruption of stronger foam state at the core outlet. This eruption has been reported by others, especially at relatively high surfactant concentration (Apaydin and Kovscek, 2001; Simjoo et al., 2013). In our results, the stronger foam does not appear in displacements at higher foam qualities. Figure 7 illustrates this effect. At the start of the experiment, foam is at steady state with a foam quality of 99%. Liquid saturation is uniform along the core except at the inlet and outlet sections. After foam quality is reduced to 96%, holding the same total superficial velocity, a stronger foam forms near the core outlet and slowly propagates upstream, as illustrated in the S_w profiles at 4.3 and 6.1 pore volumes injected. Finally, steady state is achieved after 35 pore volumes injected. S_w in the final steady-state foam, with $f_g = 96\%$, is lower than the initial S_w of the steady-state foam with $f_g = 99\%$, especially near the outlet of the core, reflecting the stronger foam state.
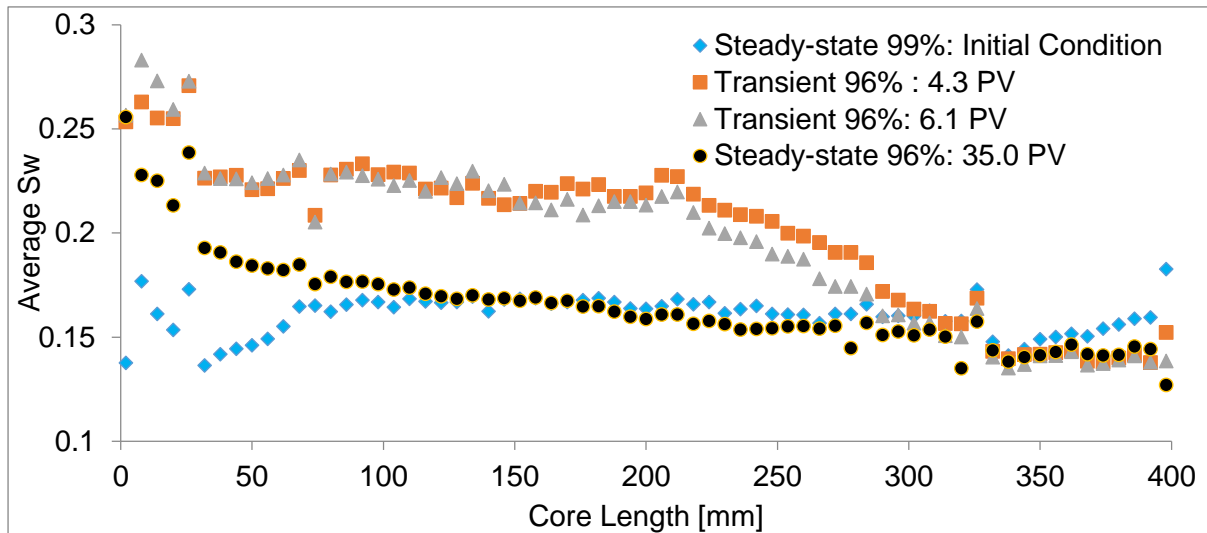

Figure 7 *Average cross-section water-saturation S_w along the core during displacements at two foam qualities. The direction of the flow is from left to right. The decline in S_w with time at 96% foam quality shows a slow upstream propagation of stronger foam.*

In every non-monotonic case, with different C_s and u_t, there had been an eruption of stronger foam at the core outlet at mid ranges of f_w but not at the driest conditions. In our experiments, the non-monotonic behaviour is independent of the initial condition. If the initial condition lies at lower water fractional-flow than that at which transition from strong foam to weak foam occurs (i.e., S_w increases as f_w decreases), $f_w \approx 0.05$ in Figure 9, and next injection condition is at greater f_w, we see this eruption again. Let the water fractional flow at which S_w begins to increase with decreasing f_w (approx. 0.05 in Fig. 6) be denoted the transition water fraction, f_{wt}. When we took consecutive data at water fractional flow greater than f_{wt}, we did not observe a *new* eruption of a stronger foam state, but that stronger state had erupted earlier and filled the core during an earlier first displacement with $f_w > f_{wt}$. As a result, attaining steady state was faster when starting from a 'wet' initial condition, $f_w = 0.9 >> f_{wt}$. because the slow upstream propagation of the stronger foam was not needed during the given displacement. This is confirmed by both S_w and pressure-gradient measurements. Figure 8 shows that the final steady-state sectional pressure drops are achieved considerably faster when the displacement by foam with $f_w = 0.05 > f_{wt}$ is started with an initial state with $f_w = 0.9$ rather than $f_w = 0.01$.

Figure 9 depicts a non-monotonic fractional-flow curve. For illustration purposes, we upscale these data using fractional-flow theory. To that end, we construct the shock for the effective fractional-flow. This construction is illustrated in Figure 9, also. We define apparent viscosity as $\mu_{app} \equiv [k \, \Delta P / (L \, u_t)]$, where k and L denote rock permeability and the length of the core section, respectively. The apparent viscosity predicted for the shock is approximately equal of 0.06 (Pa s) (60 cp) which corresponds to a mobility of $\lambda_{shock}=16.6$ [Pa s]$^{-1}$. This mobility ratio is still favourable for displacing water (viscosity 0.8 cp under these conditions) at 100% saturation, but mobility is much greater than if the shock had been to a point of tangency at larger f_w, as shown schematically in Fig. 1. Moreover, our experiments

were conducted under conditions nearly ideal for foam stability: a clean, high-permeability core, relatively low salinity, relatively low temperature, no oil present, etc. Obtaining successful mobility control under more demanding conditions in the field would be more challenging,
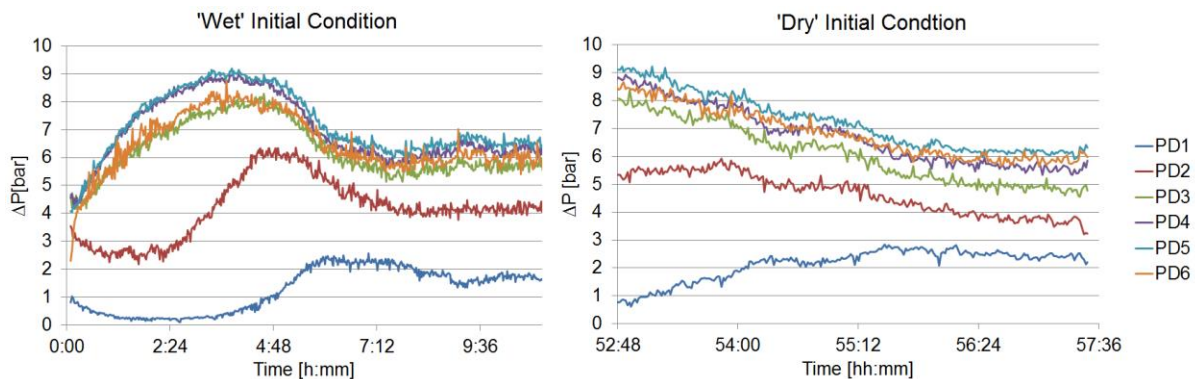

Figure 8 *Sectional differential pressures in bars as function of time in two coreflood experiments with identical injection conditions but different initial conditions. The nominal foam quality and total superficial velocity and the surfactant concentration of this experiment are 95%, 4.25 ft/day and 0.5 wt%, respectively. On the left, steady state is achieved after 8 hours when the experiment is started from a 'wet' initial condition, $f_w=0.9$. In contrast, steady state is achieved only after 55 hours when starting from a 'dry' initial condition, $f_w =0.01$, right.*
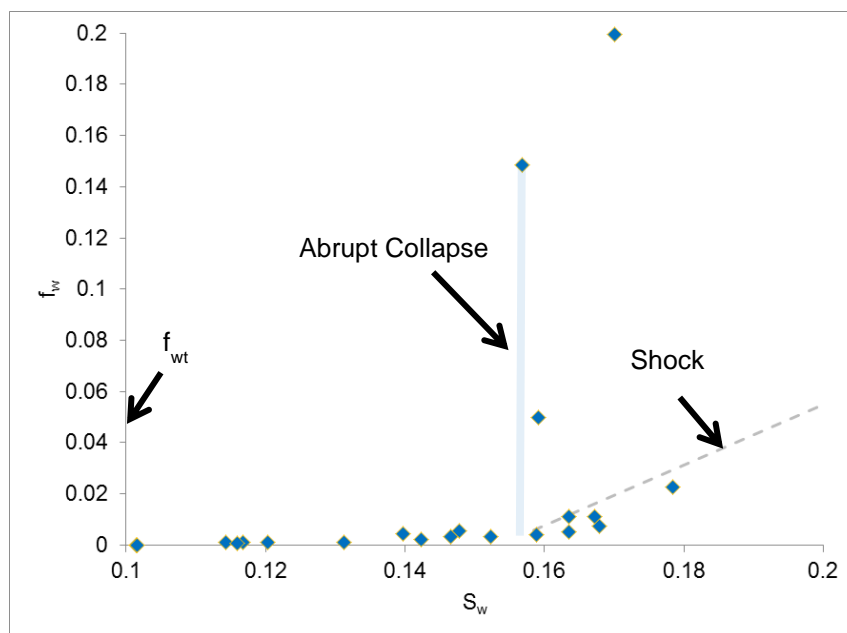

Figure 9 *Fractional flow as function of water saturation for one non-monotonic set of data. u_t and C_s are equal to 1.5×10^{-5} m/s and 0.5 wt% AOS, respectively. We plot the shock as a dashed line according to the solution method of Rossen and Bruining (2007). f_{wt} denotes the fractional flow at which S_w starts to increase with decreasing f_w.*

Table 1 summarizes our results. At the lowest C_s and u_t we did not see the eruption of a stronger foam state at the core outlet. Increasing C_s is linked in our experiments to an extension of the stronger state to lower f_w. (i.e., a reduction in transition water fraction f_{wt}). Increasing C_s, even far above the CMC, increases lamella stability in porous media (Apaydin and Kovscek, 2001; Eftekhari et al., 2017). In the same way, our results indicate that increasing superficial velocity also reduces the value of f_{wt}. Increasing superficial velocity promotes lamella creation (Gauglitz et al., 2002; Kam and Rossen,

2003). These results suggest that the stronger state depends on a shifting balance between lamella stability and lamella creation (cf. Ashoori et al, 2012; Yu et al., 2019a,b).

Table 1 *Summary of Experimental Findings, f_{wt} denotes the fractional flow at which S_w starts to increase with decreasing f_w.*

C_S (wt%)	u_t (m/s, ft/d)	Monotonic at steady state?	Transition water fraction (f_{wt})
0.037	2.94×10^{-6}, 0.83	Yes	N/A
0.037	1.5×10^{-5}, 4.25	No	0.17
0.1	1.5×10^{-5}, 4.25	No	0.17
0.1	3.0×10^{-5}, 8.50	No	0.14
0.5	1.5×10^{-5}, 4.25	No	0.05
1.0	1.5×10^{-5}, 4.25	No	0.03

Discussion

The experiments examined here are limited to a single surfactant and core type, though surfactant concentration, superficial velocity and foam quality to vary. Demonstrating the generality of the results requires further study. Previous studies (Wassmuth et al., 1994; Kibodeaux and Rossen, 1997; Xu and Rossen, 2004; Boeije and Rossen, 2018) did not specifically address possible origins of non-monotonic $f_w(S_w)$ behaviour. Close examination of those studies is needed to see if their results are consistent with our findings.

In this study, every example of a non-monotonic fractional-flow curve began with the eruption of a strong foam state at the core outlet - at least arguably, an experimental artefact of the capillary end effect in a laboratory-scale coreflood (Apaydin and Kovscek, 2001). In addition, when this occurred, the resulting stronger-foam state did not show the invariance of ∇p with gas expansion along the core (cf. Fig. 4 left and right and Fig. 5) expected in the high-quality regime (Alvarez et al., 2001). It is possible that the stronger foam that erupts is in the low-quality regime, or that it is some state not consistent with either regime. However the increase in steady-state ∇p as one approaches the core outlet (Fig. 4, right) at least suggests the possibility that this lower-mobility state within the core remains, even at steady state, dependent on the capillary end effect at the end of the core. Moreover, the relevance of the capillary end effect to field application of foam is uncertain, although similar effects can occur at reservoir heterogeneities (Falls et al., 1988; Tanzil et al., 2002; Shah et al., 2018, 2019). It is at least plausible that the coreflood data relevant to a SAG process in the field are those unaffected by the capillary end effect. In our study, we could obtain data excluding this effect either at low surfactant concentration or by using data from pre-generated foam, propagating at apparent local equilibrium (Fig. 4 left) before foam breakthrough at the core outlet. In a companion paper in preparation we scale up our monotonic $f_w(S_w)$ data sets for hypothetical field applications.

Our finding of a transition from this stronger foam to a weaker foam state as f_w decreases agrees with research on foam generation (Yu et al., 2019a), propagation (Ashoori et al., 2012; Yu et al., 2019b) and collapse (Kam and Rossen, 2003; Yu et al., 2019b). Specifically, maintenance and propagation of a strong-foam state depends on both lamella-creation mechanisms (affected in this case by superficial velocity and pressure gradient) and lamella stability (affected in this case by f_w and surfactant concentration). However, much current modelling of foam is based on the idea of a single strong-foam state that is regulated by pore size and the limiting capillary pressure P_c* (Khatib et al., 1988; Rossen and Zhou, 1995; Alvarez et al., 2001). If there are two steady states of strong foam, this raises the question: which is regulated by P_c*? What regulates the other state?

Modelling (Kam and Rossen, 2003) and experimental (Gauglitz et al., 2002) studies that now accommodate multiple foam steady states predict an abrupt transition from a strong-foam state with decreasing superficial velocity to a state of nearly complete foam collapse. The model of Lotfollahi et al. (2017) allows for multiple strong-foam states in that a stronger foam state may be locked in as velocity is reduced. Our laboratory data suggest a gradual transition, over a range of f_w, to a state of distinctly weaker strong foam. We are unaware of a model that predicts this behaviour.

Our data indicate monotonic $f_w(S_w)$ behaviour at the lowest surfactant concentrations. These concentrations are below those usually proposed for field application. However our laboratory conditions (low temperature, mild salinity, clean, water-wet rock, absence of oil) are ideal for strong foam. Under more challenging conditions in many field applications, the behaviour at higher surfactant concentrations may be closer to those we see at low concentration (and hence reduced foam stability in porous media).

Conclusions

In this study, every case of non-monotonic $f_w(S_w)$ data began with eruption of a much-stronger foam state at the time of foam breakthrough at the core outlet, an apparent result of the capillary end effect.

The importance and generality of this finding requires further study with a wider range of surfactant formulations and experimental conditions and a close examination of previous work, especially behaviour before attainment of steady state. At this point, the relevance of laboratory data taken subsequent to this event is uncertain. In this study, if foam eruption at breakthrough occurred at the core outlet, we were able to obtain monotonic $f_w(S_w)$ data by injecting pregenerated foam and taking data before foam breakthrough. No such precaution was needed at the lowest surfactant concentrations tested.

The transition from a stronger to a weaker foam state with decreasing superficial velocity and lower foam quality is consistent with modelling of foam generation, propagation and collapse. It does raise the question which steady state is most relevant to field application, and how both steady states can be consistent with the concept of a single limiting capillary pressure at a given surfactant concentration and superficial velocity.

Non-monotonicity in $f_w(S_w)$ was correctly inferred from pressure-gradient data using the water-relative-permeability function, even in cases where that function did not predict the absolute value of water saturation correctly.

Acknowledgements

References

Al Ayesh, A. H., Salazar, R., Farajzadeh, R., Vincent-Bonnieu, S., and Rossen, W. R., "Foam Diversion in Heterogeneous Reservoirs: Effect of Permeability and Injection Method," SPE Journal 22, 1402-1415 (2017); doi.org/10.2118/179650-PA

Alvarez, J. M., Rivas, H., and Rossen, W.R., "A Unified Model for Steady-State Foam Behavior at High and Low Foam Qualities," SPE Journal 6 (2001), 325-333; doi.org/10.2118/74141-PA

Apaydin, O.G. and Kovscek, A.R. "Surfactant Concentration and End Effects on Foam Flow in Porous Media," Transport in Porous Media 43, 511-536 (2001); doi.org/10.1023/A:1010740811277

Ashoori, E., Marchesin, D., and Rossen, W.R., "Multiple Foam States and Long-Distance Foam Propagation in Porous Media," SPE Journal 17, 1231-45 (2012); doi.org/10.2118/154024-PA

Boeije, C. S., and Rossen, W. R., "SAG foam flooding in carbonate rocks," J. Petroleum Science and Engineering 171, 843-853 11 (2018); doi.org/10.1016/j.petrol.2018.08.017

Eftekhari, A. A. and Farajzadeh, R., "Effect of Foam on Liquid Phase Mobility in Porous Media," Scientific Reports (2017); doi.org/10.1038/srep43870

Falls, A. H. Hirasaki, G. J., Patzek, T. W., Gauglitz, D. A., Miller, D. D., and Raulowski, T., "Development of a Mechanistic Foam Simulator: The Population Balance and Generation by Snap-Off,", SPERE 3, 884-892 (1988); doi.org/10.2118/14961-PA

Farajzadeh, R., Eftekhari, A. A., Kahrobaei, S., Hajibeygi, van der Meer, H. J., Vincent-Bonnieu, S., and Rossen, W. R., "Simulation of Instabilities and Fingering in Surfactant Alternating Gas (SAG) Foam Enhanced Oil Recovery," J. Natural Gas Sci. Eng. 34, 1191-1204 (2016); doi.org/10.1016/j.jngse.2016.08.008

Gauglitz, P.A., Friedmann, F., Kam, S. I, and Rossen, W.R., "Foam Generation in Homogeneous Porous Media," Chem. Eng. Sci. 57, 4037-4052 (2002); doi.org/10.1016/S0009-2509(02)00340-8

Heller, J. P.. "CO2 Foams in Enhanced Oil Recovery," in Foams: Fundamentals and Applications in the Petroleum Industry, L.L Schramm, ed.,Advances in Chemistry, American Chemical Society, 201-234 (1994); doi.org/10.1021/ba-1994-0242.ch005

Kam, S. I., and Rossen, W. R., "A Model for Foam Generation in Homogeneous Porous Media," SPE Journal 8 417-425 (2003); doi.org/10.1016/S0009-2509(02)00340-8

Kapetas, L., Vincent-Bonnieu, S., Farajzadeh, R., Eftekhari, A.A., Mohd Shafian, S.R., Kamarul Bahrim, R.Z. and Rossen, W.R. "Effect of permeability on foam-model parameters: An integrated approach from core-flood experiments through to foam diversion calculations," Colloids and Surfaces A: Physicochemical and Engineering Aspects 530, 172-180 (2017); doi.org/10.1016/j.colsurfa.2017.06.060

Khatib, Z. I., Hirasaki, G. J., & Falls, A. H. "Effects of Capillary Pressure on Coalescence and Phase Mobilities in Foams Flowing Through Porous Media," SPE Reservoir Eng. 3,919-926 (1988); doi:10.2118/15442-PA

Kibodeaux, K.R. and Rossen, W.R. "Coreflood Study of Surfactant-Alternating-Gas Foam Processes: Implications for Field Design". SPE Western Regional Meeting, (SPE paper 38318), Long Beach, CA, USA, 25-27 (1997); doi.org/10.2118/38318-MS

Lotfollahi, M., Kim, I., Beygi, M. R., Worthen, A. J., Huh, C., Johnston, K. P., Wheeler, M. F., and. DiCarlo, D. A., "Foam Generation Hysteresis in Porous Media: Experiments and New Insights," Transp Porous Med 116, 687–703 (2017); doi.org/10.1007/s11242-016-0796-6

Matthews, C. S.. "Carbon Dioxide Flooding," in Developments in Petroleum Science, ed. E. C. Donaldson, G. V. Chilingarian and T. F. Yen, Elsevier, 129-156 (1989); doi.org/10.1016/S0376-7361(08)70458-8

Rossen, W. R., and Bruining, J., "Foam Displacements With Multiple Steady States," SPE Journal 12, 5-18 (2007); doi.org/10.2118/89397-PA

Rossen, W.R. and Gauglitz, P.A., "Percolation Theory of Creation and Mobilization of Foams in Porous Media," AIChE J. 36, 1176-1188 (1990); doi.org/10.1002/aic.690360807

Rossen, W.R. and Zhou, Z.H., "Modeling Foam Mobility at the Limiting Capillary Pressure," SPE Adv. Technol. 3, 146-152 (1995); doi.org/10.2118/22627-PA

Schramm, L. L. "Foams: Fundamentals and Applications in the Petroleum Industry". Number 242 in Advances in Chemistry Series. American Chemical Society, Washington, DC, USA (1994); doi.org/10.1021/ba-1994-0242.fw001

Shah, S. Y., Wolf, K.-H.; Pilus, R., and Rossen, W. R., "Foam generation by capillary snap-off in flow across a sharp permeability transition," paper SPE 190210 presented at the SPE Improved Oil Recovery Conference held in Tulsa, Oklahoma, USA, 14-18 April 2018; accepted for publication in SPE Journal; doi.org/10.2118/190210-PA

Shah, S.Y, As Syukri, Wolf, K.-H., Pilus, R., and Rossen, W.R., "Foam generation by snap-off in flow across a sharp permeability transition," presented at the EAGE IOR Symposium, Pau, France, April 8-10, 2019.

Shan, D. and Rossen, W.R., "Optimal Injection Strategies for Foam IOR," SPE Journal 9, 132-150 (2004); doi.org/10.2118/88811-PA

Simjoo, M., Dong, Y., Andrianov, A., Talanana, M. and Zitha, P. L. J. "CT Scan Study of Immiscible Foam Flow in Porous Media for Enhancing Oil Recovery," Industrial & Engineering Chemistry Research 52 (18), 6221-6233 (2013); doi.org/10.1021/ie300603v

Tanzil, D., Hirasaki, G. J., & Miller, C. A., "Conditions for Foam Generation in Homogeneous Porous Media," Presented at the SPE/DOE Improved Oil Recovery Symposium, Tulsa, Oklahoma, 13-17 April (2002); doi.org/10.2118/75176-MS

Van der Meer, J., Farajzadeh, R., Rossen, B. & Jansen, J. D., "Influence of foam on the stability characteristics of immiscible flow in porous media," Physics of Fluids 30, 1 (2018); doi.org/10.1063/1.5000891

Wassmuth, F. R., Green, K. A., Randall, L., "Details of In-Situ Foam Propagation Exposed With Magnetic Resonance Imaging". SPE Reservoir Evaluation & Engineering 4, 135-145 (2001); doi.org/10.2118/71300-PA

Xu, Q. and Rossen, W. R. "Experimental Study of Gas Injection in Surfactant-Alternating-Gas Foam Process," SPE Reservoir Evaluation & Engineering, 7, 438–448 (2004); doi.org/10.2118/84183-MS

Yu, G., Rossen, W. R., and Vincent-Bonnieu, S., "Coreflood Study of Effect of Surfactant Concentration on Foam Generation in Porous Media," Journal of Industrial & Engineering Chemistry (2019a); doi.org/10.1021/acs.iecr.8b03141

Yu, G., Vincent-Bonnieu, S., and Rossen, W. R., "Foam Propagation at Low Superficial Velocity: Implications for Long-Distance Foam Propagation," presented at the EAGE IOR Symposium, Pau, France, April 8-10, 2019b.

Zhou, Z.H. and Rossen, W.R., "Applying Fractional-Flow Theory to Foams for Diversion in Matrix Acidization," SPE Prod. Fac. 9, 29-35 (1994); doi.org/10.2118/24660-PA